http://hdl.handle.net/1765/111020

Erasmus MC
Universitair Medisch Centrum Rotterdam

Some controversies in endovenous laser ablation of varicose veins addressed by optical-thermal mathematical modeling

Anna Poluektova
Wendy Malskat
Martin van Gemert
Marc Vuylsteke
Cornelis Bruijninckx
Martino Neumann
Cees van der Geld

Lasers Med Sci; 2014 Mar;29(2):441-52

Erasmus University Rotterdam

ABSTRACT

Minimally invasive treatment of varicose veins by endovenous laser ablation (EVLA) becomes more and more popular. However, despite significant research efforts performed during the last years, there is still a lack of agreement regarding EVLA mechanisms and therapeutic strategies. The aim of this article is to address some of these controversies by utilizing optical-thermal mathematical modeling.

Our model combines Mordon's light-absorption based optical-thermal model with the thermal consequences of the thin carbonized blood layer on the laser fiber tip that is heated up to temperatures of around 1000°C due to the absorption of about 45% of the laser light. Computations were made in MATLAB. Laser wavelengths included were 810, 840, 940, 980, 1064, 1320, 1470 and 1950 nm. We addressed: The effect of direct light absorption by the vein wall on temperature behavior, comparing computations using normal and zero wall absorption; Predicting the influence of wavelength on the temperature behavior; The effect of the hot carbonized blood layer surrounding the fiber tip on temperature behavior, comparing wall temperatures from using a hot fiber tip and one kept at room temperature; The effect of blood emptying the vein, simulated by reducing the inside vein diameter from 3 down to 0.8 mm; The contribution of absorbed light energy to the increase in total energy at the inner vein wall in the time period where the highest inner wall temperature was reached; The effect of laser power and pullback velocity on wall temperature of a 2 mm inner diameter vein, at a power/velocity ratio of 30 J/cm at 1470 nm; A comparison of model outcomes and clinical findings of EVLA procedures at 810 nm, 11 W and 1.25 mm/s, and 1470 nm, 6 W and 1 mm/s.

Interestingly, our model predicts that the dominating mechanism for heating up the vein wall is *not* direct absorption of the laser light by the vein wall but heat flow to the vein wall and its subsequent temperature increase from two independent heat sources. The first is the exceedingly hot carbonized layer covering the fiber tip; the second is the hot blood surrounding the fiber tip, heated up by direct absorption of the laser light. Both mechanisms are about equally effective for all laser wavelengths. Therefore, our model concurs Vuylsteke et al.'s finding of more circumferential vein wall injury in veins (nearly) devoid of blood, but it does not support their proposed explanation of direct light absorption by the vein wall. Furthermore, EVLA appears to be a more efficient therapy by the combination of higher laser power and faster pullback velocity than by the inverse combination. Our findings suggest that 1470 nm achieves the highest EVLA efficacy compared to the shorter wavelengths at all vein diameters considered. However, 1950 nm EVLA is more efficacious than 1470 nm albeit only at very small inner vein diameters (smaller than about 1 mm, i.e. veins quite devoid of blood). Our model confirms the efficacy of both clinical procedures at 810 and 1470 nm.

In conclusion, our model simulations suggest that direct light absorption by the vein wall is relatively unimportant, despite being the supposed mechanism of action of EVLA that drove the introduction of new lasers with different wavelengths. Consequently, the presumed advantage of wavelengths targeting water rather than hemoglobin is flawed. Finally, the model predicts that EVLA therapy may be optimized by using 1470 nm laser light, emptying of the vein before treatment, and combining a higher laser power with a greater fiber tip pullback velocity.

INTRODUCTION

Minimally invasive treatment of varicose veins by endovenous laser ablation (EVLA) has become a widely used clinical method because of its high efficacy and low complication rate. Guided by the general consensus that irreversible injury of the vein wall by sufficient temperature increase is the therapeutic goal to be achieved, performed research during the past years still has not provided agreement regarding the mechanisms by which this injury is reached and which laser power setting and pullback velocity is optimal in reaching this goal effectively and safe (1, 2). So far, four EVLA mechanisms of action that produce an increase in vein wall temperature have been proposed: 1. Direct contact between laser fiber tip and vein wall (3). 2. The optical-thermal interaction between the laser light emitted out of the fiber and the surrounding tissues. First, the laser light power is redistributed over the surrounding blood, vein wall and perivenous tissue by absorption and scattering. Subsequently these structures are being heated up by the combined effects of absorbed laser light power and heat flows that develop between locations of higher and lower temperatures (4, 5) 3. Heat flowing from the exceedingly hot layer of carbonized blood around the laser fiber tip, diffusing through the blood and reaching and heating up the vein wall (6, 7). 4. Heat transfer from boiling bubbles to the vein wall. These steam bubbles most likely originate in tiny pores of the hot carbonized layer but also in the blood when the blood temperature exceeds the threshold for boiling. They subsequently propagate a few cm distal from the tip before condensing and transferring their energy to blood and vein wall (8-10).

The exact contribution of these mechanisms in achieving EVLA efficacy is unknown (1, 2). Equally so, there is no consented best therapeutic strategy, clearly demonstrated by the large variety of laser wavelengths, laser power settings, pullback velocities and degree of blood emptying of treated veins that are currently in clinical use (1, 3). The available and clinically used wavelengths vary from 810 nm to 1470 nm. The hemoglobin molecules in red blood cells are the absorption target of the shorter wavelengths (810 nm, 940 nm, 980 nm and 1064 nm) and the water molecules in the endothelial cells the assumed target of the longer wavelengths (1320 nm and 1470 nm) (11, 12). We also included 1950 nm, this wavelength is absorbed about three times better in blood and vein wall than 1470 nm and has therefore been touted to be an interesting wavelength for EVLA therapy (12)

In this article, we address some of the existing controversies by utilizing our optical-thermal mathematical model (13). The first controversy concerns the question whether the increased amount of circumferential vein wall destruction at 1470 nm EVLA and at smaller inner vein diameters (1, 2), can be explained by direct light absorption of the vein wall (4), by heat conduction-related mechanisms from the hot fiber tip, or by both (4, 6). The second concerns the question whether EVLA efficacy increases at lower or

higher laser power and pullback velocity combinations. The third whether laser wavelength affects the EVLA modes of action (1, 2, 4, 6, 7, 10, 14) The latter addresses the controversy whether EVLA at wavelengths targeting water rather than hemoglobin are advantageous (11, 12).

METHODS

Our model (13) combines Mordon's optical-thermal model of light absorption (4) with the thermal consequences of the thin layer of carbonized blood (6), always covering the laser fiber tip and which absorbs about 45% of the laser light before it reaches the surrounding blood (7). The effects of steam bubbles, their propagation and condensation centimeters distal to the fiber tip has been approximately accounted for in the model by increasing the thermal conductivity of blood by a factor of 200 when the blood temperature exceeds 95°C (13). Although this mitigates the calculated blood temperatures to about 100°C, temperatures in excess of that value do occur. We assumed a vein temperature of 20°C following administration of tumescent anesthesia before switching on the laser power, accounting for the fact that the tumescent fluid is kept in the refrigerator before it is administrated by multiple injections around the vein at body temperature.

The geometry used in the simulations is presented in Figure 1. It consists of a cylindrical blood vessel with wall and perivenous tissue with a length of L = 200 mm. The total radius of the considered (mathematical) domain is R = 10 mm. The inner radius, *ri*, of the vein is varied between 0.4 and 1.5 mm. The outer radius, *r0*, is 1 mm larger than *ri*, accounting for a vein wall thickness of 1 mm. The laser fiber tip, with a radius of *rfiber* =

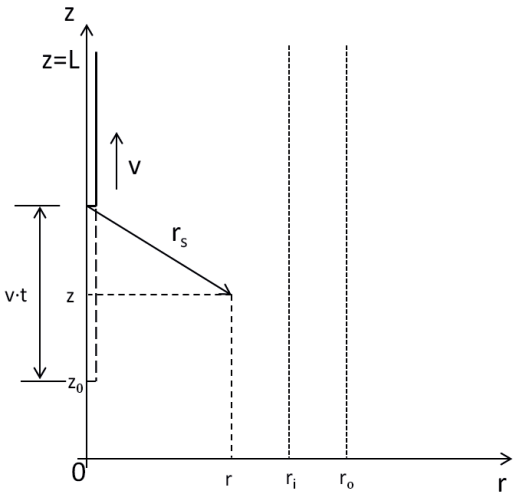

Figure 1. Geometry of vein and fiber with r_i and r_o the inner and outer radii of the vein, z_0 = 20 mm, temperature evaluation is at z = 40 mm. Not to scale.

0.3 mm, is centered within the vessel, at $r = 0$, and moves up in axial direction, z, with a constant velocity, v, varied between 1 and 4 mm/s. At time $t = 0$, the fiber tip is located at axial coordinate $z0 = 0.1L = 20$ mm. We have chosen $z0 = 20$ mm instead of 0 mm to allow heat to flow in the distal direction too when, at time $t = 0$, the laser is switched on and pulling back of the fiber begins at a constant velocity of v mm/s. At time t, the fiber tip is at axial position $z = z0 + v \cdot t$. The laser light is entering the fiber tip with power, P, varying between 3 and 25 W, and because 45% is absorbed by the carbonized layer of blood, the remaining 55% is emitted out of the fiber into the blood (i.e. between 1.65 and 13.75 W).

The observation point where we will evaluate the computed temperatures is at axial coordinate $z = 0.2L = 40$ mm just inside the vein wall. Thus, at e.g. $v = 2$ mm/s, the fiber tip reaches the observation point 10 s after switching on the laser and starting the withdrawal of the fiber (Figure 2).

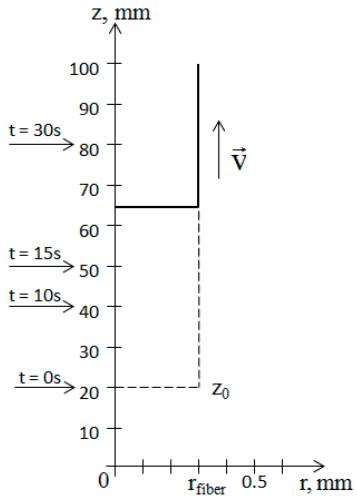

Figure 2. The axial location of the fiber tip over time for v = 2 mm/s.

The thermal properties of blood, vein wall and perivenous tissue, i.e. thermal conductivity, k, mass density, ρ, heat capacity at constant pressure, cp, and thermal diffusivity, a, are summarized in Table 1. Their optical properties, i.e. absorption coefficient, μa, and reduced scattering coefficient, $\mu's$, are presented in Table 2. The data for all wavelengths but 1950 nm come from the original model (13). For 1950 nm, the blood and vessel wall absorption are from the same source (13); the reduced scattering coefficient of vessel wall comes from an extrapolation of the $\mu's$ of skin, from Zonios and Demou (15), as displayed in Figure 4B of Lister et al. (16). For blood, the reduced scattering coefficient is an extrapolation from the value at 1470 nm assuming the same ratio at 1470 versus 1950 nm as for the vein wall. The other parameters are from Vuylsteke and Mordon (1).

Table 1. Thermal properties

Symbol	Unit	Fiber	Blood	Vein wall and perivenous tissue
k	[W/m°C]	1.3	0.6	0.56
ρ	[kg/m3]	2400	1000	1050
c_p	[J/kg°C]	703	4181	3780
$\alpha = k/(\rho \cdot c_p)$	[m2/s]	7.7·10-7	1.43·10-7	1.41·10-7

k, thermal conductivity; ρ, density; c_p heat capacity at constant pressure; α, thermal diffusivity

The mathematical formulation of the problem is briefly explained in Appendix 1. Details can be found elsewhere (13). All calculations were made for laser wavelengths of 810 nm, 840 nm, 940 nm, 980 nm, 1064 nm, 1320 nm, 1470 nm and 1950 nm. However, to keep the number of Figures practicable we will present most of the results for 810 and 1470 nm only, because the temperature effects caused by 810 nm appeared to be representative for all shorter wavelengths, including 1320 nm, and the 1470 nm results are representative for 1950 nm as well.

The mathematical model evaluates the temperature behavior in the blood, vein wall, perivenous tissue and the carbonized blood layer. The model therefore allows studying the influence on calculated temperatures of relevant clinical settings, e.g. by varying the laser wavelength, laser power, degree of collapse of the treated vein, and pullback velocity. However, it also permits establishing the influence on the wall temperature of factors such as absorption of the vein wall and temperature of the hot fiber tip. We studied the following issues.

Table 2. Optical properties

	μa [1/mm]			μ's [1/mm]		
λ [nm]	Blood	Vein wall	Perivenous tissue	Blood	Vein wall	Perivenous tissue
810	0.21	0.2	0.017	0.73	2.4	1.2
840	0.21	0.18	0.019	0.75	2.33	1.18
940	0.28	0.12	0.027	0.64	2.13	1.1
980	0.21	0.1	0.030	0.6	2.0	1.0
1064	0.12	0.12	0.034	0.58	1.95	0.98
1320	0.3	0.3	0.045	0.54	1.8	0.9
1470	3.0	2.4	0.35	0.52	1.7	0.84
1950	10.0	7.5	0.35	0.30	1.0	0.15

λ, wavelengths; μ_a, absorption coefficient; μ'_s, reduced scattering coefficient

The effect of vein wall absorption of laser light on the inner vein wall temperature

The contribution of directly absorbed laser light by the vein wall to the inner vein wall temperature follows from comparing computations with normal vein wall absorption (see Table 2), and simulated zero absorption of the vein wall and surrounding perivenous tissue. The simulations were performed for an inner radius of the vein of ri = 1.5 mm, power P = 15 W, and velocity v = 2 mm/s.

The effect of wavelength on the inner vein wall temperature

The simulations were performed as before, only the inner vein diameter varied from 0.8 to 3 mm.

The effect of the hot carbonized blood layer on the inner vein wall temperature

The contribution of the hot fiber tip to the inner vein wall temperature follows from comparing computations with normal vein wall absorption and including that 45% of the emitted laser power is absorbed by the carbonized blood layer on the fiber tip (7), and normal vein wall absorption but keeping the fiber tip at body temperature despite also including the 45% power reduction of the emitted laser light. The simulations were performed with the same parameters as before.

The effect of blood emptying of the vein on the inner vein wall temperature

Grades of blood emptying of the vein by Trendelenburg positioning of the patient and introduction of tumescent anesthetic fluid into the great saphenous vein compartment was mimicked by varying the inside vein diameter from respectively 0.8, 1, 1.5, 2, 2.5 to 3 mm. Considering that fiber tips normally measure 0.6 mm, a diameter of 0.8 mm mimics a nearly totally collapsed vein, and a diameter of 3 mm a rather small vein.

Contribution of the absorbed light energy to the increase in total energy at the inner vein wall while reaching the highest temperature

Equation (A.2) of Appendix 1 describes the amount of light power absorbed in an infinitesimally small tissue volume located at radial coordinate r from the fiber tip and at time t. We choose this infinitesimal volume just inside the inner vein wall, at z = 40 mm and $r = r_i$. Then, integrating Eq. (A.2) over the time period between $t = 0$ and $t = t_{end}$, where t_{end} is the time at which the inner wall temperature reaches its maximum value, gives the total energy of the absorbed light in that small infinitesimal volume in this time period, denoted by $E_{light}(r_i, t_{end})$ (J/vol). We compare this to the total increase in energy in that infinitesimal volume in the same period of time, $E_{total}(r_i, t_{end})$. Appendix 2 gives the details.

The effect of emitted laser power and pullback velocity on the inner vein wall temperature

We varied the laser power at 3, 6 and 12 W, and proportionately the pullback velocity at 1, 2 and 4 mm/s respectively, at a power/velocity ratio of 30 J/cm, at 1470 nm and 2 mm inner vein diameter (12).

Comparison of model outcome and clinical findings of two EVLA procedures

We simulated two clinical procedures of EVLA, performed at the Helder Clinic (by CMAB). The first is at 810 nm, 11 W, 1.25 mm/s pullback velocity, the second at 1470 nm, 6 W and 1 mm/s. In these simulations, the axial coordinate of the initial fiber tip position was at $z0 = 0.1 \cdot L = 10$ mm and the observation point at $z = 0.2 \cdot L = 20$ mm. For better comparison with the clinical findings, the inner vein radius was set to 1 mm and the outer radius to 2 mm, based on the ultrasound findings. Comparison was with ultrasound pictures obtained during the procedures.

RESULTS

The effect of vein wall absorption of laser light on the inner vein wall temperature

Figure 3 shows the temperature profiles at the inner vein wall (at $ri = 1.5$ mm) as a function of time at axial position $z = 40$ mm. The lines show the results for the case with normal vein wall absorption, the lines with symbols correspond to the case with simulated zero vein wall absorption.

For both normal and zero wall absorption, the temperature at the vein wall reaches the same maximum value and virtually at the same time for each of the wavelengths. For 810 nm, the maximum vein wall temperature is 104°C reached at $t_{end} = 10.8$ s and for 1470 nm it is 109°C reached at 10.6 s. Over time, the curves for normal and zero vein wall absorption show only very small differences at 810 nm, implying that the scattered light that is directly absorbed by the vein wall does not play an important role in the mechanism of induced temperature compared to the heat flow from the hot fiber tip and heated blood toward the vein wall. The temperature profiles for 1470 nm are exactly the same for both cases (with and without vein wall absorption). It confirms that, at 1470 nm and 3 mm inner vein diameter, virtually no photons reach the vein wall for absorption.

The effect of wavelength on the inner vein wall temperature

Figure 4 shows computations of the inner vein wall temperature versus wavelength, at inner vein diameters varying between 0.8, 1, 1.5, 2, 2.5 and 3 mm. Interestingly, a higher

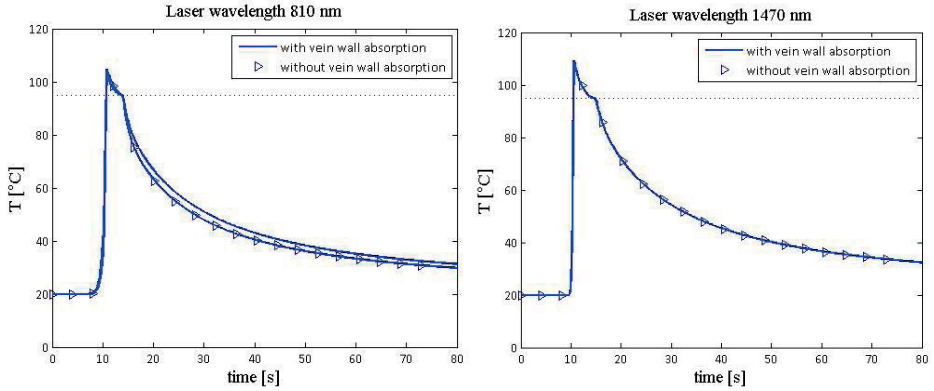

Figure 3. Temperature profiles at the inner vein wall, 3 mm diameter, as a function of time, with vein wall absorption (lines) and without vein wall absorption (lines with symbols), at 810 nm (left) and 1470 nm (right), at 15 W, 2 mm/s.

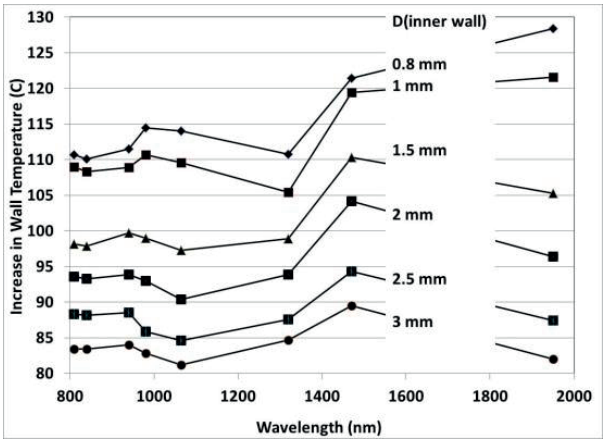

Figure 4. Increase in the inner vein wall temperature versus wavelength for inner vein diameters of 0.8, 1, 1.5, 2, 2.5 and 3 mm, at 15 W, 2 mm/s.

EVLA efficacy is predicted at 1470 nm compared to EVLA with the shorter wavelengths, for all vein diameters considered. For very small vein diameters (0.8 and 1 mm), our model predicts a slightly larger inner vein wall temperature at 1950 nm EVLA than at 1470 nm, a consequence of the higher temperature of the carbonized blood layer of about 111°C (1084°C at 1470 nm versus 1195°C at 1950 nm, see also Figure 6 below) and, less importantly, of the (very) small fraction of the light that reaches the vein wall.

The effect of the hot carbonized blood layer on the inner vein wall temperature

Figure 5 shows the contribution of the hot tip to the temperature at the inner vein wall at $z = 40$ mm as a function of time, at 810 nm and 1470 nm, using a 3 mm diameter, 15 W and 2 mm/s. Lines indicate the model with the hot tip included, and lines with symbols the model with the tip kept at room temperature.

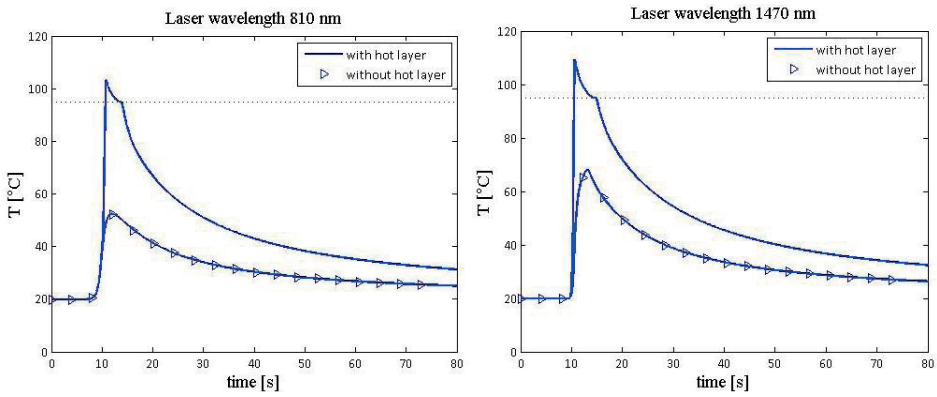

Figure 5. Temperature profiles at the inner vein wall with a diameter of 3 mm, as a function of time, with the hot tip (lines) and with the tip kept at room temperature (lines with symbols) at 810 nm (left) and 1470 nm (right). P = 15 W, v = 2 mm/s.

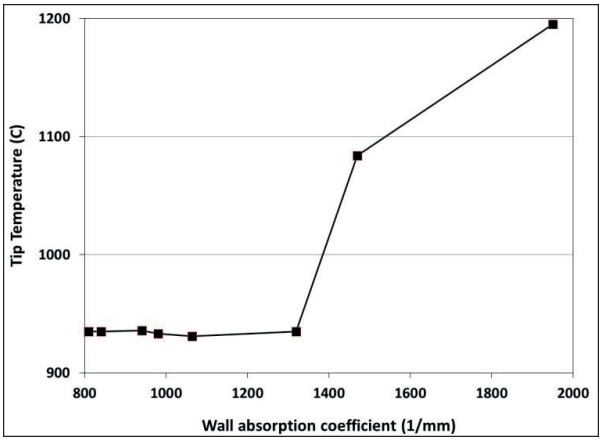

Figure 6 shows the computed temperatures at the fiber tip as a function of wavelength, at 15 W and 2 mm/s. The results were found to be independent of the

Figure 5 shows a quite interesting and we believe unexpected phenomenon. First, when the hot tip is included, the computed temperature rise at the inner vein wall is more than twice as large compared to when the tip is kept at room temperature. Remarkably, however, our model predicts that there is still a significant rise in temperature, despite keeping the fiber tip at room temperature and despite the results displayed in Figure 3, which show that this temperature rise cannot come from direct absorbed laser light by the vein wall. The mechanism responsible here is the thermal effect induced by direct absorption of the emitted laser light by the surrounding blood, causing heating up of the blood, first beginning close to the fiber tip and subsequently propagating to the vein wall as a heat flow, leading to the increase in wall temperature. This mechanism is also included in Mordon's model (4).

The effect of blood emptying of the vein on the inner vein wall temperature

The calculations for different vein wall inner diameters (0.8 mm, 1 mm, 1.5 mm, 2 mm, 2.5 mm, 3 mm), the smaller diameters mimicking blood emptying of the vein, were made for all wavelengths. We included computations with direct light absorption by a normal and by a zero absorbing vein wall, and presence and absence of a hot tip.

Figure 7 shows an example of temperature profiles at the vein wall, at 1470 nm, for two inner vein diameters (0.8 mm, left curve, and 2.5 mm, right curve), as a function of time. The solid lines indicate the temperatures in the normal situation, with 45% of power absorbed by the hot carbonized layer around the fiber tip, and the remaining power (55%) absorbed by the blood, vein wall and surrounding tissue. The dashed lines with symbols indicate the temperatures with *zero* vein wall absorption. The solid lines with symbols indicate the temperatures with the fiber tip kept at room temperature. For an inner vein diameter of 2.5 mm (right curves) there is no difference between the model computations with and without vein wall absorption, implying that the plain line and the dashed line with symbols overlap. Again, this is due to fact that virtually no photons reach the vein wall at a distance of ≥ 1 mm from the tip (Figure 3). For a distance of 0.4 mm or smaller (inner vein diameter ≤ 0.8 mm), a few photons reach the vein wall and become absorbed, giving rise to a very small and clinically insignificant increase in temperature. However, the other mechanisms of heating up the vein wall during EVLA, i.e. heat flow toward the vein wall from the hot fiber tip and from the hot blood around the fiber tip, identified above (Figure 5), occur much stronger at well emptied veins (diameter below 1.5 mm, see also Figure 8).

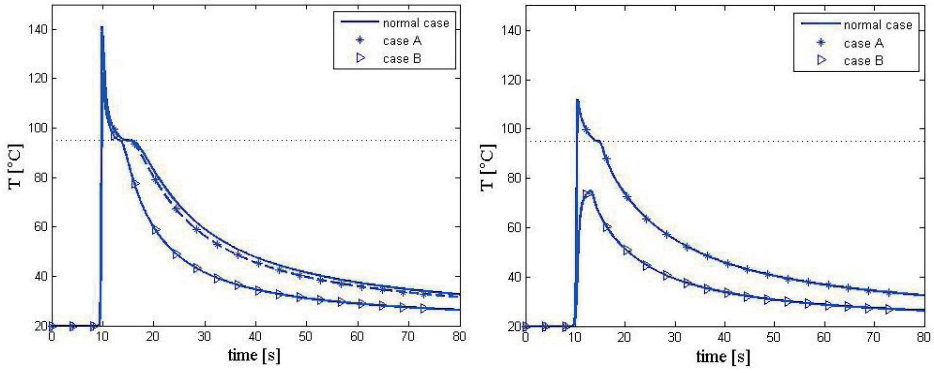

Figure 7. Temperature profiles at 1470 nm for two inner vein diameters, 0.8 mm (left) and 2.5 mm (right). Case A: results with zero vein wall absorption. Case B: results with the fiber tip kept at room temperature.

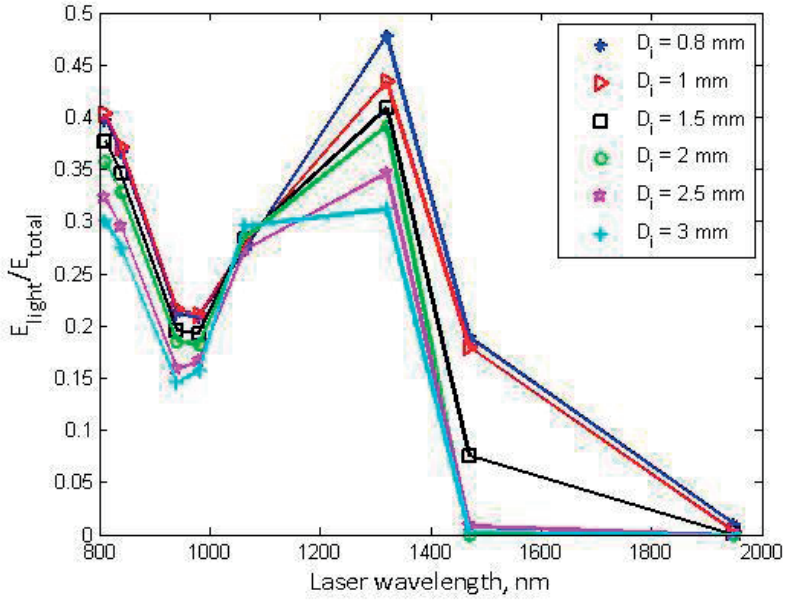

Figure 8. Laser wavelength dependence of E_{light}/E_{total}, calculated at the inner vein wall at z = 40 mm, for different inner vein wall diameters D_i.

Contribution of the absorbed light energy to the increase in total energy at the inner vein wall while reaching the highest temperature

Figure 8 shows the computed ratio E_{light}/E_{total} for all wavelengths and vein diameters used. It is a measure of the contribution of the absorbed laser light energy, relative to the increase in total energy, in an infinitesimally small volume element just inside the vein wall, during the time period between laser onset and reaching the maximum inner wall temperature. Figure 8 suggests that direct light absorption by the vein wall plays some role in the heating up of the wall for EVLA at 810, 940, 980, 1064 and 1320 nm, albeit only contributing between about 15% and 50%. Using 1470 nm EVLA, it contributes almost 20%, provided the vein is (nearly) totally collapsed. At 1950 nm EVLA, direct absorption of the laser light by the vein wall contributes virtually nothing to the increase in inner wall temperature.

The effect of emitted laser power and pullback velocity on wall temperature

Figure 9 shows computed inner vein wall temperatures versus laser power, at 1470 nm and 2 mm diameter, for a power/velocity ratio of 30 J/cm, previously used clinically (12). It is clearly shown that the highest inner vein wall temperature corresponds to a power of 12 W and a pullback velocity of 4 mm/s in the EVLA setting chosen for the simulations.

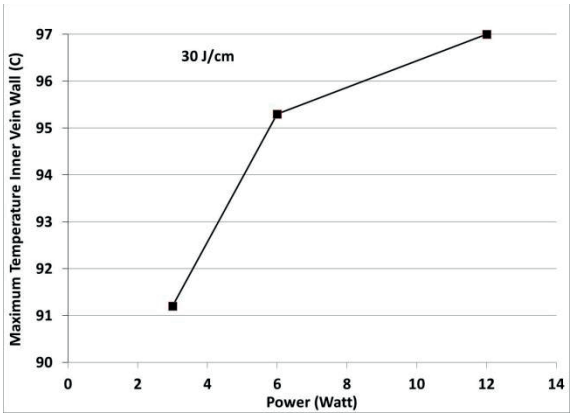

Figure 9. Maximum inner vein wall temperatures at 1470 nm and various laser powers (3, 6 and 12 W) and pull-back velocities (1, 2 and 4 mm/s), at a power/velocity ratio of 30 J/cm.

Comparison of model outcome and clinical findings of two EVLA procedures

Figure 10 shows the computed results for the two clinical EVLA cases of, first, 810 nm, 11 W, 1.25 mm/s pullback velocity (left curves), and, second, 1470 nm, 6 W and 1 mm/s (right curves). Figure 11 shows ultrasound pictures following these procedures. Although the calculated predictions at 810 and 1470 nm both suggest full coagulation of the entire vessel wall, the 810 nm model predictions suggest slightly better efficacy, because the calculated maximum temperature at the outer wall, although high enough for irreversible injury, is about 13°C higher at 810 nm than at 1470 nm. Nevertheless, ultrasonography suggests the inverse, a more intense injury at 1470 than at 810 nm. A possible explanation for this observation is that the two treatments were evaluated with two different ultrasound machines and that the displayed reflection pattern, the ultrasound picture, depends on the parameters set for ultrasound focusing and contrast, but also on the native reflectivity of individual tissue structures, e.g. fat separating membranes and air bubbles in the tumescent liquid.

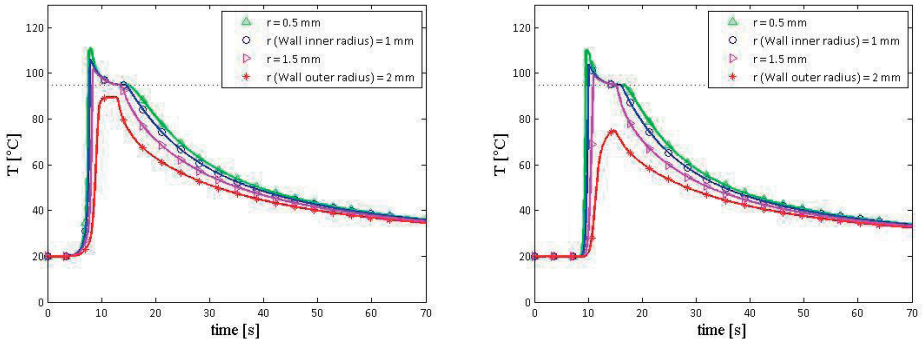

Figure 10. Temperature profiles as a function of time using a 2 mm inner vein wall diameter. Left curve: 810 nm, 11 W, 1.25 mm/s. Right curve: 1470 nm, 6 W, 1 mm/s.

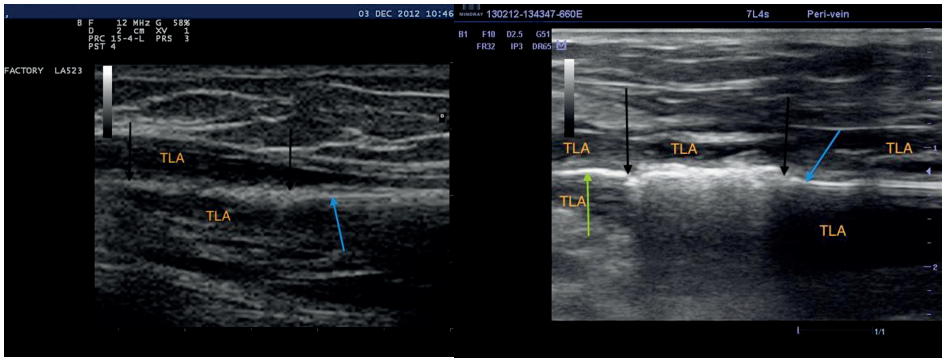

Figure 11. (Left) Ultrasound image of the central Great Saphenous Vein (GSV), about 8 s after starting EVLA at 810 nm. Blue arrow indicates the fiber tip. Part of the GSV between the black arrows just has been treated. TLA is the tumescent local anesthesia surrounding the GSV. Note that, compared to 1470 nm EVLA, lesser echogenicity of the GSV remnant. (Right) Ultrasound image of the central GSV, just 10 seconds after starting EVLA at 1470 nm. The segment of about 1 cm between the black arrows was treated; the fiber tip is at the point of the blue arrow. Left of the left black arrow, marked by a green arrow, a white line with a diameter of about 1 mm is visible, presumably caused by steam bubbles escaping into the common femoral vein. The untreated vein wall is visible around the fiber tip as grey lines, the treated vein wall as a linear and irregular but markedly echogenic structure.

DISCUSSION

Surprisingly, our model predicts that direct absorption of laser light by the vein wall is not the dominating contributor to the efficacy of simulated EVLA procedures. For example, at a very small, 0.8 mm, inner vein diameter, direct light absorption contributes a 47% maximum to the wall temperature at 1320 nm, but less than 20% at 1470 nm and about 1% at 1950 nm. At a more realistic diameter of about 1.5 - 2 mm (Figure 11), these numbers are about 37% at 1320 nm and virtually zero at 1470 and 1950 nm. Instead, the predicted leading mechanism is that two independent heat diffusion flows begin at the fiber tip, propagate through the blood to the vein wall and, after arrival, heat up the vein wall. The two heat sources that produce these heat flows and contribute about equally to the increase in vein wall temperature are the exceedingly hot fiber tip, as well as the hot blood surrounding the fiber tip, heated up by direct absorption of the emitted laser light out of the tip. This finding gives an interesting turn to the hypothesis of Vuylsteke and Mordon, that direct light absorption by the vein wall causes increased levels of circumferential vein wall destruction in blood emptied veins (1). Our model confirms their experimental finding in Figure 4 but, instead, the proposed mechanism by our model is that the heat flows from the hot tip and heated blood to the vein wall, as already explained in this paragraph. Additionally, it gives an equally interesting outlook on the past multiple introductions of new EVLA wavelengths, which were all based on increasing the direct absorption of laser light by the vein wall by "bypassing" absorption of the

light by hemoglobin. Our results thus firmly confirm the statement made by Vuylsteke and Mordon that classification into hemoglobin- and water-absorbed wavelengths is flawed (1). The results also suggest that 1950 nm, with very large absorption in water and blood, proposed to be an interesting future EVLA candidate, perhaps even requiring less tumescent anesthesia (12), will actually not be superior to 1470 nm.

Obviously, modeling such complex and coupled action mechanisms as in EVLA procedures performed in patients with individual variability in anatomy and pathophysiology cannot identify all possible events that may occur. However, the importance as well as limitation of this type of computational modeling has been expressed well by Brown et al. (17), in their paper on allometric scaling laws of mammalian circulatory systems, stating that (converted to EVLA) "like any model, it is a deliberate oversimplification that can serve as a point of departure for understanding a much more complicated (EVLA) reality. It should be useful if it captures the essence of the mechanisms that underlie EVLA". Particularly, our model relies on the accuracy of the optical and thermal parameters used. Although the absorption behavior of blood is well known below about 1000 nm and above 1400 nm, taking the latter equal to the absorption of water, it is not in the spectral in-between. The reduced scattering properties of blood in the spectral band beyond 1000 nm, needed for EVLA modeling, are not well known. For example, previous work showed that the large absorption peaks in the visible part of the spectrum causes related peaks in the scattering behavior (18). This mechanism likely occurs too at the strong water absorption peaks around 1500 and 1900 nm but it is not taken into account in the behavior of the reduced scattering coefficients yet. In addition, it is well known that the optical properties of blood also depend on the temperature (19), which was not taken into account in our model and neither in Mordon's model (4). We hypothesize that the thermal properties used for blood, vessel wall and perivenous tissue are more accurate than the optical properties, due to the large fraction of water included in soft tissues and blood, and the accurately known thermal properties of water.

A more fundamental issue is that the model does not fully capture the effects of steam bubbles by just increasing the thermal conductivity of blood by a factor of 200 at temperatures above 95°C. We are currently including the effects of steam bubbles more thoroughly using computational fluid dynamics methodology, which however requires solving several coupled partial differential equations, including the Navier-Stokes equation. Another approximation (in Mordon's as well as our model) is neglecting possible changes in the shape of the vein wall when tumescent anesthesia is administrated because this may cause thickening of the wall due to spasms but also an increased tissue pressure by pressing the wall to be fold around the catheter surface. However, we anticipate that the pressure is such that the vein wall volume remains homogeneous for absorption and scattering of the laser light. Besides, even if this is not exactly so, our

results will unlikely change significantly because of the relative unimportance of direct vein wall absorption of the laser light.

Our EVLA model, as well as Mordon's model, uses cylinder symmetry of the vein with the fiber centered in the middle. This geometry precludes studying the possible effects of EVLA with a bare fiber, the geometry often used in clinical practice, including the consequences of direct contact between fiber tip and vein wall. Although direct contact was the first proposed mechanism of action of EVLA efficacy, by Navarro et al. (3), we hypothesize that it is insufficient to achieve permanent closure of most varicose veins.

An important model finding of the new identified mechanism is the suggestion that 1470 nm achieves a higher inner vein wall temperature, hence a better EVLA efficacy, than all shorter wavelengths considered, at all inner vein diameters examined. This outcome at least confirms hitherto unproven opinions of many clinicians. It implies that the 1470 nm EVLA laser power can be lowered, predicted by about 10% compared to the power used at other wavelengths, at identical pullback velocity, and still obtaining the same EVLA efficacy. Our model also suggests that combining higher laser power with faster pullback velocity is more effective than the opposite at equal J/cm. The 1950 nm EVLA is only more efficient than 1470 nm for very small inner vein diameters, smaller than about 1 mm. However, the incomplete account of steam bubbles in the present model makes these predictions to remain slightly tentative.

In conclusion, our model simulations suggest that: 1. Direct absorption of laser light by the vein wall is relatively unimportant; previously, the presumed importance of this mechanism supported the unfounded introduction of so-called 'water targeting laser wavelengths' 2. EVLA classification between hemoglobin and water absorbed wavelengths is flawed (1) 3. EVLA procedures may be optimized by using 1470 nm laser light, (nearly) complete blood emptying of the vein, and combining a higher laser power with a higher pullback velocity of the fiber tip.

REFERENCES

1. Vuylsteke ME, Mordon SR. Endovenous laser ablation: a review of mechanisms of action. Ann Vasc Surg 2012;26:424-433.
2. Van Gemert MJC, van der Geld CWM, Bruijninckx CMA, Verdaasdonk RM, Neumann HAM. Comment to Vuylsteke ME and Mordon SR. Endovenous laser ablation: a review of mechanisms of action. Ann Vasc Surg 2012;26:424-33. Ann Vasc Surg 2012;26:881-883.
3. Navarro L, Navarro N, Salat CB, Gomez JF, Min RJ. Endovascular laser device and treatment of varicose veins. US 6,398,777 B1, patent filed in 1999, granted in 2002.
4. Mordon SR, Wassmer B, Zemmouri J. Mathematical modeling of 980-nm and 1320-nm endovenous laser treatment. Lasers Surg Med 2007; 39:256-65.
5. Welch AJ, van Gemert MJC (Editors). Optical-thermal response of laser-irradiated tissue. 2nd edition, Springer, Dordrecht, 2011.
6. van den Bos RR, Kokaert MA, Neumann HAM, Bremmer RH, Nijsten T, van Gemert MJC. Heat conduction from the exceedingly hot fiber tip contributes to the endovenous laser ablation of varicose veins. Lasers Med Sci 2009;24:247-251. Erratum Lasers Med Sci 2009;24:679.
7. Amzayyb M, van den Bos RR, Kodach VM, de Bruin DM, Nijsten T, Neumann HAM, van Gemert MJC. Carbonised blood deposited on fibers during 810, 940 and 1,470 nm endovenous laser ablation: thickness and absorption by optical coherence tomography. Lasers Med Sci 2010;25:439-447.
8. Proebstle TM, Lehr HA, Kargl A, Espinola-Klein C, Rother W, Bethge S, Knop J. Endovenous treatment of the greater saphenous vein with a 940-nm diode laser: thrombotic occlusion after endoluminal thermal damage by laser-generated steam bubbles. J Vasc Surg 2002;35:729–736.
9. Disselhof BCVM, Rem AI, Verdaasdonk RM, der Kinderen DJ, Moll FL. Endovenous laser ablation: an experimental study on the mechanism of action. Phlebology 2008;23:69-76.
10. van der Geld CWM, van den Bos RR, van Ruijven PWM, Nijsten T, Neumann HAM, van Gemert MJC. The heat-pipe resembling action of boiling bubbles in endovenous laser ablation. Lasers Med Sci 2010;25:907-909.
11. Goldman MP, Mauricio M, Rao J. Intravascular 1320-nm laser closure of the great saphenous vein: a 6- to 12-month follow-up study. Dermatol Surg 2004;30:1380-1385.
12. Almeida J, Mackay E, Javier J, Mauriello J, Raines J. Saphenous laser ablation at 1470 nm targets the vein wall, not blood. Vasc Endovascular Surg 2009;43:467-472.
13. Van Ruijven PWM, Poluektova AA, van Gemert MJC, Neumann HAM, Nijsten T, van der Geld CWM. Optical-thermal mathematical model for Endovenous Laser Ablation of varicose veins. Lasers Med Sci 2014;.(Special Issue, in press)
14. van den Bos RR, van Ruijven PWM, van der Geld CWM, van Gemert MJC, Neumann HAM, Nijsten T. Endovenous simulated laser experiments at 940 nm and 1470 nm suggest wavelength independent temperature profiles. Eur J Vasc Endovasc Surg 2012;44:77-81.
15. Zonios G, Dimou A. Modeling diffuse reflectance from semi-infinite turbid media: application to the study of skin optical properties. Optics Express 2006;14:8661-8674.
16. Lister T, Wright PA, Chappell PH. Optical properties of human skin. J Biomed Opt 2012;17:090901 (1-15).
17. Brown JH, EnquistBJ, West GB. Allometric scaling laws in biology. Science 1997;278:369-373.
18. Faber DJ, Aalders MCG, Mik EG, Hooper B, van Gemert MJC, van Leeuwen TG. Oxygen saturation dependent absorption and scattering of blood. Phys Rev Lett 2004;93:028102 (1-4).
19. Barton JK. dynamic changes in optical properties. In: Welch AJ, van Gemert MJC (editors). Optical-thermal response of laser-irradiated tissue, 2nd edition, Springer, 2011, Chapter 9.

APPENDIX 1

The mathematical formulation of the heat conduction governed by Fourier's law supplemented with appropriate boundary and initial conditions is given by

$$\rho c \frac{\partial T}{\partial t} = \nabla \cdot (k \nabla T) + q(r, z, t) \qquad at \quad (r, z) \in \Omega, t \geq 0, \tag{A.1}$$

$$q = \frac{0.55 \cdot P \mu_a}{4\pi D_{dif} \sqrt{(r^2 + (z - z_0 - v \cdot t)^2)}} \exp(-\mu_{eff} \sqrt{(r^2 + (z - z_0 - v \cdot t)^2)}), \tag{A.2}$$

$$q(z, 0 \leq r \leq r_{fiber}) = q_{tip} = \frac{0.45 \cdot P}{V_{tip}}, \tag{A.3}$$

$$T(r_{int}^-, z, t) = T(r_{int}^+, z, t) \qquad if \; 0 \leq z \leq L, \quad t \geq 0, \tag{A.4}$$

$$(k \frac{\partial T}{\partial r}) \; (r_{int}^-, z, t) = (k \frac{\partial T}{\partial r}) \; (r_{int}^+, z, t) \qquad if \; 0 \leq z \leq L, \quad t \geq 0, \tag{A.5}$$

$$\frac{\partial T}{\partial t}(r, z, t) = 0 \qquad if \; r = 0 \vee R, 0 \leq z \leq L, \quad t \geq 0, \tag{A.6}$$

$$\frac{\partial T}{\partial t}(r, z, t) = 0 \qquad if \; 0 \leq r \leq R, z = 0 \vee L, \quad t \geq 0, \tag{A.7}$$

$$T(r, z, 0) = T_{initial} = 293[K] \qquad at \; (r, z) \in \Omega \tag{A.8}$$

with q the volumetric heat generation given by the product of absorption coefficient and fluence rate (W/m3) (5) μa the absorption coefficient (1/m), μs the scattering coefficient (1/m) and g the average cosine of the scattering angle (the anisotropy factor), *rfiber* the fiber radius (m), *Vtip* the volume of the carbonized layer (m3), which thickness is about 0.1 mm and does not change during the computation. We assumed that 45% of the light propagating towards the fiber tip is absorbed by the carbonized layer (6).

The rectangular computational domain is described by $\Omega = \{(r, z) \; R^2 | \, , 0 \leq r \leq R, \; 0 \leq z \leq L$, where R is the radial size of the computational domain (m), and L the axial size of the computational domain (m). The optical parameters such as reduced scattering coefficient (μ_s'), the optical diffusion constant (D_{dif}) and the effective attenuation coefficient (μ_{eff}) are defined by

$$\mu_s' = \mu_s(1 - g) \tag{A.9}$$

$$D_{dif} = \frac{1}{3(\mu_s' + \mu_a)} \tag{A.10}$$

$$\mu_{eff} = \sqrt{3\mu_a(\mu_s' + \mu_a)} \tag{A.11}$$

This model is discussed in detail elsewhere (13).

APPENDIX 2

The amount of volumetric light energy absorbed at the inner vein wall at z = 40 mm and $r = r_i$, in the time period between $t = 0$ and $t = t_{end}$, where t_{end} is the time at which the inner wall temperature reaches its maximum value, $E_{light}(r_i, t_{end})$, is given by

$$E_{light}(r_i, t_{end}) = \int_0^{t_{end}} \mu_a(r_i)\varphi^*(r_i, t)dt \text{ where } \varphi^*(r, t) = \begin{cases} \varphi(r, t), & \frac{dT}{dt} \geq 0 \\ 0, & \frac{dT}{dt} < 0 \end{cases} \quad (B.1)$$

$\mu_a(r_i)$ is the light absorption coefficient and $\varphi(r_i, t)$ the fluence rate (W/m^2) of the vein wall at point r_i and time t and product $\mu_a(r_i)\varphi(r_i, t)dV$ is the absorbed power in an infinitesimally small volume dV centered at r_i, t; the reason not to consider times when the time rate of change of the temperature is negative is explained below. In the same period of time, from $t = 0$ to $t = t_{end}$, the total volumetric increase in energy, $E_{total}(r_i, t_{end})$, is given by

$$E_{total}(r_i, t_{end}) = \int_0^{t_{end}} \rho c_p \left.\frac{dT(r_i, t)}{dt}\right|^+ dt = \rho c_p[T(r_i, t_{end}) - T(r_i, t = 0)] \quad (B.2)$$

$\left.\frac{dT}{dt}\right|^+$ indicates the positive value of the derivative, which by definition is zero when the time rate of change of temperature is negative. At the latter times, no heat is accumulated at the point ri, which may imply that heat diffusion exceeds radiation power absorbation at these times. These times are simply not considered. As a consequence, the RHS of (B.2) is actually a summation of integrals over periods of time when the time rate of change of the temperature is positive. Ratio E_{light} / E_{total} has been computed for all wavelengths and vein diameters used.